ELSEVIER

European Journal of Pharmacology 394 (2000) 171–179

ejp

www.elsevier.nl/locate/ejphar

Properties of Ca^{2+} release-activated Ca^{2+} channel block by 5-nitro-2-(3-phenylpropylamino)-benzoic acid in Jurkat cells

Jack H. Li, Katherine T. Spence, Pauline G. Dargis, Edward P. Christian *

Department of CNS Discovery, AstraZeneca Pharmaceuticals, Wilmington, DE 19850-5437, USA

Received 8 February 2000; accepted 15 February 2000

Abstract

Ca^{2+} release-activated Ca^{2+} current (I_{crac}) has been previously characterized biophysically in Jurkat lymphocytes and other non-excitable cells, but pharmacology remains poorly developed. The present objective was to delineate with whole cell recording details of the interaction of the chloride channel blocker, 5-nitro-2-(3-phenylpropylamino)-benzoic acid (NPPB), with I_{crac} in Jurkat cells. NPPB reversibly inhibited I_{crac} in a concentration-dependent manner ($IC_{50} = 5\ \mu M$). Kinetics for block and unblock of I_{crac} by NPPB indicated a bimolecular interaction. Michaelis–Menten analysis indicated that NPPB interacts competitively with extracellular Ca^{2+} permeating the I_{crac} pathway. Finally, analysis of the pH dependence of I_{crac} block by NPPB revealed a reduction in the apparent affinity during extracellular alkalinization that based on the pK_a for NPPB, suggested that the neutral form of NPPB blocks the Ca^{2+} release-activated Ca^{2+} (CRAC) channel. Taken together, our results suggest a direct interaction between NPPB and the CRAC channel, and should help guide insights for developing novel and more selective analogues.

Keywords: NPPB (5-nitro-2-(3-phenylpropylamino)-benzoic acid); Patch clamp; Ca^{2+} current; Ca^{2+} current, Capacitative; Ca^{2+} release-activated current; Jurkat cell; pH Modulation

1. Introduction

Ca^{2+} release-activated Ca^{2+} (CRAC) current (I_{crac}) is a small, but highly selective Ca^{2+} current that has been identified and characterized at the electrophysiological level in various non-excitable cell types such as mast cells, macrophages and T lymphocytes (for review, see Lewis, 1999). Based on both noise analysis (Zweifach and Lewis, 1993; Lepple-Wienhues and Cahalan, 1996), and single channel recordings with a monovalent charge carrier (Kerschbaum and Cahalan, 1999), evidence has accumulated that the I_{crac} pathway is subserved in physiological saline by an ion channel (CRAC channel) of exceedingly small conductance (on the order of fS), rather than an alternative ion transport mechanism. A defining feature of I_{crac} is that activation of the CRAC channel is linked necessarily to depletion of intracellular Ca^{2+} stores by diverse manipulations such as: (1) direct chelation of free cytosolic Ca^{2+}; (2) prevention of store refilling through inhibition of Ca^{2+} transporting ATPase; or (3) activation of microsomal IP_3 receptors with mitogens (Zweifach and Lewis, 1993). However, the mechanism coupling store depletion to channel activation remains equivocal.

The CRAC channel provides the major pathway for sustained Ca^{2+} influx in T cells during mitogenic stimulation (Zweifach and Lewis, 1993; Premack et al., 1994) and has been implicated as critical to T cell activation (Chung et al., 1994). More generally, the ability to modulate this pathway has been linked to the control of diverse cellular functions such as secretion and cell proliferation (for review, see Lewis, 1999).

Although the proposed physiological roles of the CRAC channel also infer considerable potential as a point for therapeutic intervention, these hypotheses have only received indirect support based primarily on manipulations with a limited choice of poorly selective pharmacological agents: selective, high affinity blockers of this pathway are virtually lacking. In addition, there is little information concerning the blocking mechanism of the known moderate affinity inhibitors. Thus, these compounds may exert their effect by acting directly at the CRAC channel or alternatively by way of interfering with the poorly under-

* Corresponding author. Tel.: +1-302-886-5944; fax: +1-302-886-2766.

E-mail address: ed.christian@astrazeneca.com (E.P. Christian).

0014-2999/00/$ - see front matter
PII: S0014-2999(00)00144-8

stood I_{crac} activation pathway, or other biochemical mechanisms modulating the CRAC channel. An improved understanding of the blocking mechanisms of the currently known inhibitors would provide guidance for development of more potent and selective pharmacological tools.

Recently, Gericke et al. (1994) showed that 5-nitro-2-(3-phenylpropylamino)-benzoic acid (NPPB) inhibits I_{crac} in human endothelial cells, and Reinsprecht et al. (1995) further reported that a number of organic molecules including NPPB and NPAA (*N*-phenylanthranilic acid, also known as diphenylamine-2-carboxylic acid) inhibit I_{crac} in the RBL-2H3 rat mast cell line. Those compounds are better known for their ability to inhibit Cl^- current in a variety of epithelial tissues such as the rabbit loop of Henle, the dogfish rectal gland, the rabbit colon, the canine trachea, and the toad cornea (Wangemann et al., 1986; Greger et al., 1987, 1991; Li and Kau, 1987; McCann et al., 1989), as well as in many non-epithelial cells, including fibroblasts, human peripheral T lymphocytes, bovine pulmonary arterial endothelial cells and other non-excitable cells (Nilius et al., 1994; Heinke et al., 1995; Schumacher et al., 1995; Gschwentner et al., 1996).

The goal of the present study was to evaluate in greater depth properties of NPPB block of I_{crac} in an effort to improve more generally the understanding of pharmacological mechanisms by which inhibitors exert their effects on this channel. Thus, we demonstrated that I_{crac} in Jurkat cells was sensitive to NPPB blockade in the low micromolar range. Moreover, we have obtained data at the macroscopic level that NPPB interacts with CRAC channels with apparent 1:1 stoichiometry, and that NPPB appears to compete directly with external calcium permeating the channel. This evidence is consistent with a direct interaction of NPPB and the CRAC channel. Finally, we have obtained evidence that the uncharged form of NPPB is the relevant active species for blocking I_{crac}, based on the effect of pH in modulating inhibition. Some of these results have been published in preliminary form (Spence et al., 1996; Li et al., 1997, 1998).

2. Materials and methods

2.1. Cell culture

All studies were performed in the human leukemic E6-1 Jurkat T cell line (ATCC T1B 152). Cell cultures were maintained at log growth phase between 0.1 and 1.5×10^6 cells/ml in medium containing RPMI 1640 (Mediatech, Herndon, VA) and 10% fetal bovine serum (HyClone, Logan, UT). Cell cultures were incubated at 37°C in an atmosphere containing 5% CO_2. For recording, cells in a 150-μl aliquot of media were allowed to adhere to a poly-D-lysine-coated plastic culture dish for 3–5 min before being switched to experimental solutions.

2.2. Recording solutions

The composition of the extracellular solution was (in mM): NaCl 160, KCl 4.5, $CaCl_2$ 2, $MgCl_2$ 1, D-glucose 5, HEPES 5, pH:7.4 with NaOH, ~320 mOsm. The pipette solution included: Cs-aspartate 140, $MgCl_2$ 2, EGTA 10, HEPES 10, pH: 7.2 with CsOH, ~305 mOsm. The ''Ca^{2+}-free'' extracellular solution used to evaluate leak current in I_{crac} recordings consisted of equimolar Mg^{2+} substituted for Ca^{2+}. For recording volume-activated Cl^- current ($I_{Cl(vol)}$), external solution was changed to one diluted by 20% with deionized H_20. Solutions were filtered through 0.22-μm pore size filters and stored for up to 1 month as aliquots at 4°C (extracellular) and −20°C (intracellular solution).

NPPB (RBI, Natick, MA) was dissolved in dimethyl sulphoxide at a concentration of 5 mM and stored frozen as stock aliquots for final dissolution in extracellular buffer on the day of the experiments.

Extracellular solutions were switched with a linear array of gravity fed glass-lined tubes (100 μm i.d.; Hewlett Packard, Wilmington, DE) controlled by a system of solenoid valves (BME Systems, Baltimore, MD). The tube containing the desired solution was localized <1 cell diameter from the cell before the solenoid was activated. This system enabled complete exchange of extracellular solutions in <200 ms, based on the time course for disappearance of Ca^{2+}-selective I_{crac} upon switching to Ca^{2+}-free solution (Christian et al., 1996a).

2.3. Whole cell recording and analysis

Experiments were performed at room temperature (22–24°C) in a static bath chamber mounted on the stage of a Nikon Diaphot inverted microscope. The standard whole cell configuration of the patch clamp technique was used for recordings (Hamill et al., 1981). Pipettes were fabricated from thin wall borosilicate glass (1.5 mm o.d., 1.12 mm i.d.; World Precision Instruments, Sarasota, FL) on a Flaming-Brown P-87 Puller (Sutter Instruments, Novato, CA), fire polished to a DC resistance of 2–8 MΩ and coated with Sylgard (Dow Corning, Midland, MI) near the tip. Membrane currents were amplified with either an Axopatch 1B, 200A or 200B amplifier (Axon Instruments, Foster City, CA), low pass filtered at 1 kHz with an 8-pole Bessel filter, and then digitized at 3–5 kHz as computer files with either a TL-1 (Scientific Solutions, Solon, OH) or a Digidata 1200 interface (Axon Instruments). Voltage clamp protocols were implemented and data acquisition performed with pClamp 6.0 software (Axon Instruments). Origin software (Microcal, Northampton, MA) was used to iteratively fit various functions to the data and construct figures. Averaged data are expressed as mean ± S.E.M. For statistical tests, $p < 0.05$ was taken to denote a significant effect.

The pipette current was zeroed before a seal was formed. The resistance of the patch seals was >10 GΩ. Whole cell capacitance was nulled with circuitry in the amplifier. Following initial attainment of the whole cell configuration, and at subsequent intervals during the experiment, uncompensated capacitive current transients at the onset and offset of voltage steps of -1 mV and 10 ms duration were obtained to determine the whole cell capacitance, C_m, and the series resistance, R_s. Cells were rejected if either of these parameters varied by $>10\%$ during the experiment. Series resistance compensation was not used in most experiments. Command potentials were not corrected for the approximately -10 mV calculated junction potential (Barry and Lynch, 1991) between the standard pipette and bath solutions. None of these measurement errors were judged to have significant impact on the conclusions reached in this study.

To minimize the electrochemical gradient for Ca^{2+} influx, cells were held at a potential of 0 mV. I_{crac} was measured with repetitive (0.1-1 Hz) steps to -100 mV for 200 ms. Under these conditions, stable recordings were attainable for usually >10 min. Three to five current epochs were digitally averaged for all measurements. The current amplitude was determined in the averaged trace by further digital averaging over a 2–3-ms interval, 10 to 15 ms after the onset of the voltage step to avoid contribution by uncompensated capacitive transients and minimize CRAC channel inactivation. The magnitude of specific I_{crac} was calculated as the difference between the currents measured in the presence and in the absence of Ca^{2+} (''leak'' current; equimolar substitution by Mg^{2+}). Inhibition produced by compounds was normalized as a percentage between the control (100%) and leak current (0%) values.

$I_{Cl(vol)}$ was evaluated as current evoked during repetitive (0.1–1 Hz) 200 ms voltage ramps from -100 to $+20$ mV (0 mV holding potential), following exposure of recorded cells to hypotonic external solution. Current with this protocol remained stable generally for >10 min and could be reversed by reapplication of isosmotic solution. $I_{Cl(vol)}$ was measured by digital averaging over the interval from $+15$ to $+18$ mV.

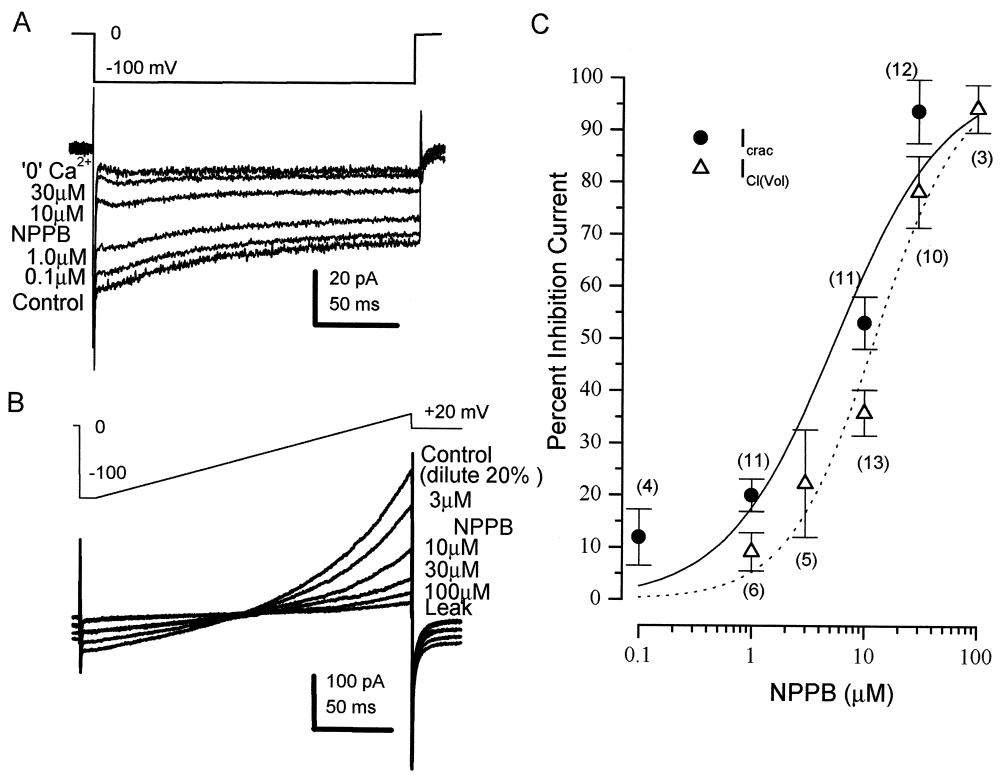

Fig. 1. Concentration-dependent inhibition by NPPBof I_{crac} and $I_{Cl(vol)}$ in Jurkat cells. (A) Superimposed traces of whole cell current responses elicited by the voltage step protocol in the upper panel, using solutions described in Section 2 for I_{crac} recording. Records were filtered at 1 kHz and digitized at 5 kHz. Each treatment is indicated to the left of the corresponding trace. The responses in figure were recorded after the effect reached a steady-state. (B) Superimposed traces of whole cell current responses elicited by the voltage ramp protocol shown (upper trace in panel), using solutions defined in Section 2 for $I_{Cl(vol)}$ recording. (C) Mean steady-state concentration–response relationships for I_{crac} and $I_{Cl(vol)}$ inhibition by NPPB. Each data point represents the mean ± S.E.M. (n in parentheses) percentage current inhibition obtained to the indicated NPPB concentration. Data were obtained with the protocols shown in panels A and B. Percentage inhibition for current in each experiment was normalized between 0% and 100% as described in Section 2. Lines (solid, I_{crac}; dashed, $I_{Cl(vol)}$) are iterative fits to a Hill equation: $100/[1+(IC_{50}/x)^{n_H}]$, where x is the NPPB concentration, IC_{50} is the concentration producing 50% current block, and n_H is the Hill coefficient. Parameters obtained by the fit were: I_{crac}, $IC_{50}=5.6$ µM; $n_H=0.9$; $I_{Cl(vol)}$, $IC_{50}=12.2$ µM; $n_H=1.1$).

3. Results

3.1. Equipotent inhibition of I_{crac} and I_{Cl} in Jurkat cells by NPPB

As previously described by several laboratories (McDonald et al., 1993; Zweifach and Lewis, 1993; Christian et al., 1996a), depletion of microsomal Ca^{2+} stores in Jurkat cells by dialyzing with Ca^{2+}-free pipette solution activated a Ca^{2+}-selective I_{crac} that reached an asymptotic amplitude over several minutes, as monitored by repeated steps to −100 mV from a 0-mV holding potential. Fig. 1A exemplifies the effects of various ionic and pharmacological manipulations on this asymptotic current. The Ca^{2+} specificity of this current was evidenced by its near abolishment when the external Ca^{2+} was substituted with equimolar Mg^{2+}. NPPB (0.1–30 μM) reduced I_{crac} in a concentration-dependent manner to nearly complete block (i.e., Mg^{2+} substitution level) at 30 μM (Fig. 1A). The mean dose–response curve constructed from a group of experiments in physiological external medium was well fitted by a Hill equation, revealing that NPPB inhibited I_{crac} with an IC_{50} of 5.6 ± 2.6 μM and Hill coefficient (n_H) of 0.9 ± 0.3 (Fig. 1C).

$I_{Cl(vol)}$ activated by cell swelling with hypotonic solution has been documented previously in Jurkat cells (Lewis et al., 1993). In agreement with this prior report, reduction of extracellular osmolality (dilution of buffer by 20%) resulted in activation of an outwardly rectifying current, as measured by repetitive voltage ramps from −100 to +20 mV (Fig. 1B). This current achieved a steady-state magnitude after several minutes of recording in dilute buffer. The current reversed near −45 mV, consistent with the predicted Cl^- reversal potential under these conditions, and thus was taken to be $I_{Cl(vol)}$. NPPB blocked $I_{Cl(vol)}$ in a concentration-dependent manner, and with a potency (IC_{50}: 12.2 ± 2.1 μM; n_H: 1.1 ± 0.2), similar to that observed for I_{crac} inhibition (Fig. 1C).

3.2. Stochiometry of I_{crac} block by NPPB

The Hill coefficient of ~1 determined from the evaluation of steady-state I_{crac} block by NPPB suggested that NPPB interacts to block I_{crac} with a non-cooperative 1:1

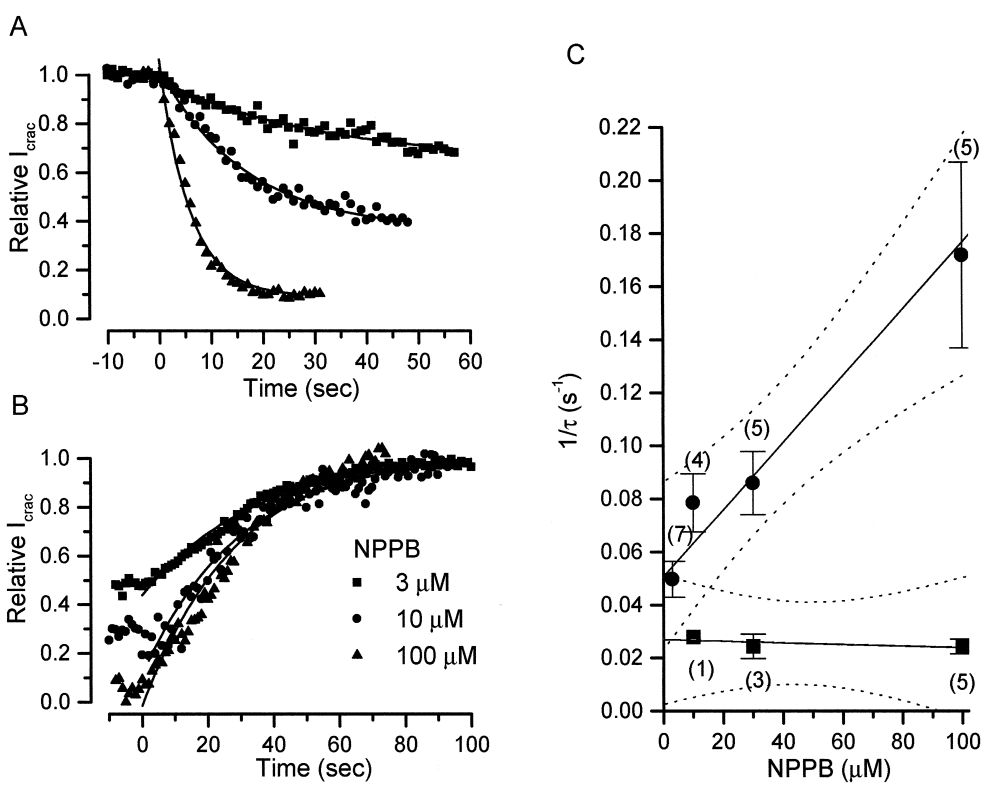

Fig. 2. Kinetic analysis of blocking and unblocking rates of I_{crac} by NPPB. (A) Concentration dependence of NPPB blocking rate. Time courses of inhibition of current were obtained from three different cells exposed to the indicated (Panel B, legend) NPPB concentrations at time 0. Current was measured by repetitive (1 Hz) 100-ms test steps to −100 mV. For this plot, I_{crac} amplitudes were normalized between the control current (1) and leak current (0) levels, as described in Section 2. Solid lines on data points are fits to a monoexponential decay function yielding a τ for each concentration. (B) Rate of recovery of I_{crac} from NPPB block at various concentrations. Format is identical to (A). (C) Plot of reciprocals of τ values for block (circles) and unblock (squares) of I_{crac} by NPPB, as a function of concentration. Data were derived using experimental protocols shown in (A) and (B). Solid lines represent linear regression fits to the data points, and dashed lines the upper and lower 95% confidence limits for each fit, based on the S.E.M.s of the data. See Section 3 for binding and unbinding rate constants derived from these fits.

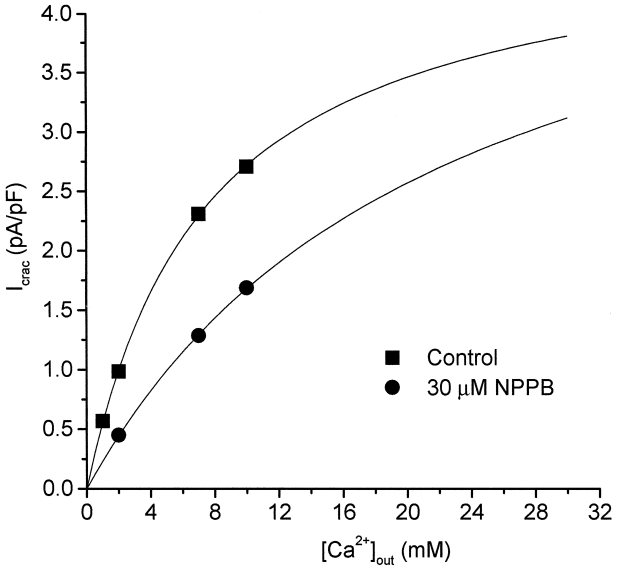

Fig. 3. Effect of extracellular Ca^{2+} concentration on inhibition of I_{crac} by NPPB. Each point represents the mean ± S.E.M. (n in parentheses) I_{crac} density obtained to the indicated $[Ca^{2+}]_{out}$ under Control conditions (squares), and in the presence of 30 μM NPPB (circles). Solid lines are iterative fits to a type of Michaelis–Menten equation of the form: $I_{crac} = I^{*}_{max}[Ca^{2+}]_{out}/\{[Ca^{2+}]_{out} + K_d\}$, where I_{max} represents the maximal current density achievable at saturating $[Ca^{2+}]_{out}$, and K_d the dissociation constant of Ca^{2+} for self-inhibiting flux through the CRAC channel. Data derived from the fits were: Control, $I_{max} = 4.9$ pA/pF, $K_d = 8.1$ mM; NPPB, $I_{max} = 4.5$ pA/pF, $K_d = 17.7$ mM.

stoichiometry. To further characterize the properties of the interaction of NPPB with the CRAC channel, a kinetic analysis of the blocking and unblocking rates was undertaken (Fig. 2). The rate of block and unblock of I_{crac} by NPPB was investigated at NPPB concentrations from 1 to 100 μM. Fig. 2A and B show that both the blocking and unblocking time courses were well described by mono-exponential kinetics. The NPPB block rate was concentration-dependent, with increasing NPPB concentration increasing the rate of block and thus decreasing the time constant. The unblocking time constant (measured in a separate set of experiments), in contrast, appeared to be concentration-independent. The reciprocal of the blocking time constant was a linear function of NPPB concentration (Fig. 2C), and linear regression yielded a binding rate constant of 1.25×10^3 M^{-1} s^{-1}. The reciprocals of the directly measured unblocking time constants were also fitted by linear regression to yield an unbinding rate constant of 0.027 s^{-1}. These kinetic measurements yielded a K_d of 21.5 μM, which was ~4-fold greater than the IC_{50} derived from the steady-state I_{crac} inhibition measurement (Fig. 1). However, since the steady-state-derived IC_{50} was inclusive within the 95% confidence bands of the regression lines fitted to reciprocal time constants, the values derived from the steady-state and kinetic measurements were not considered to be statistically distinct.

3.3. Ca^{2+}-dependence of I_{crac} inhibition by NPPB

In the rat mast cell, I_{crac} amplitude has been shown to be a saturable function of extracellular $[Ca^{2+}]$ with an apparent K_d of 3.3 mM and a Hill coefficient of 1 when measured during a −40 mV voltage step (Hoth and Penner, 1993). In the Jurkat cell, the conductance of CRAC channel shows a similar relationship to extracellular $[Ca^{2+}]$ (Premack et al., 1994). Fig. 3 confirms these reports by showing that when extracellular $[Ca^{2+}]$ was increased over several concentrations between 1 and 10 mM, I_{crac} measured during a −100 mV voltage step increased toward an asymptotic maximum. I_{crac} amplitude as a function of extracellular $[Ca^{2+}]$ was well fitted with a single-site model of Ca^{2+} self-inhibition that represents an adaptation of a formal Michaelis–Menten analysis (Fig. 3). Thus, a

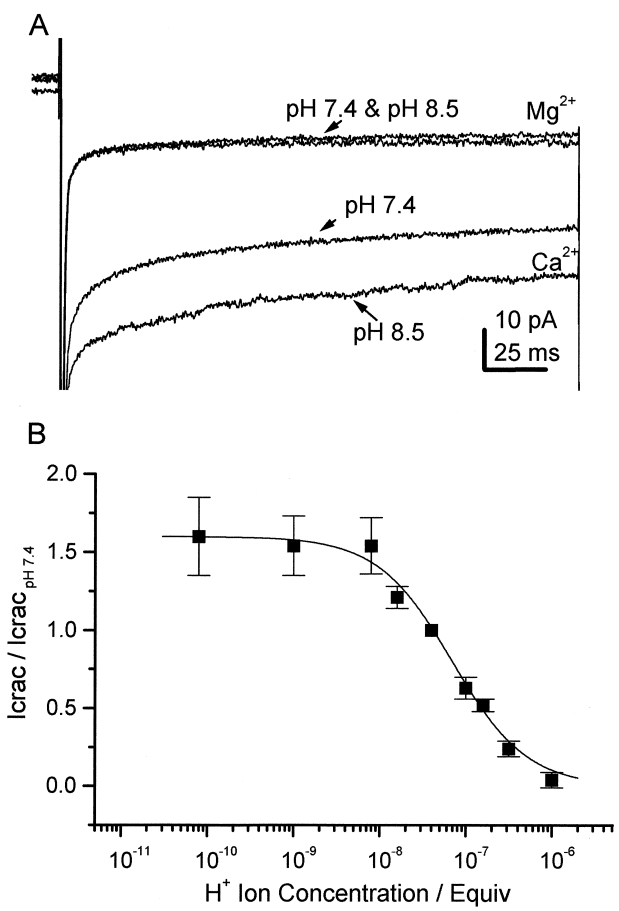

Fig. 4. Effect of external medium pH on I_{crac}. (A) Superimposed I_{crac} tracings in the presence and the absence of Ca^{2+} (equimolar replacement with Mg^{2+}) at normal external pH 7.4 and alkaline pH 8.5. Note that extracellular alkalinization increase I_{crac} in the presence of Ca^{2+} but had no effect on the background leak current labeled 'Mg^{2+}'. (B) Dependence of I_{crac} on external pH in the range of 6 to 10. The ordinate shows the amplitude of I_{crac} normalized to its value at pH 7.4. Data points represent the mean ± S.E.M. obtained from three to six experiments. The solid line represents an iterative fit to the same Hill function as in Fig. 1C. Parameters of the fit were pK_a (= pIC_{50}): 7.2 and n_H: 1.0, indicative of a single-site interaction.

maximal asymptotic I_{crac} density of 4.9 pA/pF and an apparent K_d of 8.1 mM were indicated by this analysis for cells in normal physiological buffer. The presence of 30 μM NPPB inhibited I_{crac}, but the proportion of current blocked decreased with increasing extracellular $[Ca^{2+}]$. The Michaelis–Menten analysis applied to these data (Fig. 3) revealed that NPPB did not appreciably change maximal I_{crac} density (4.5 pA/pF in NPPB), but increased the apparent K_d for Ca^{2+} block of I_{crac} from 8.1 to 17.7 mM.

3.4. pH dependence of I_{crac} inhibition by NPPB

To establish the range of pH for investigating the pH dependence of NPPB inhibition of I_{crac}, an analysis of the dependence of I_{crac} itself on external pH was first necessary. Fig. 4 shows that increasing the extracellular pH from 7.4 to 8.5 increased current magnitude. That alkalinization increased I_{crac} specifically was confirmed by the fact that the pH increase had no effect on leak current following substitution of Ca^{2+} by Mg^{2+} in the same cell (Fig. 4A). While alkalinization enhanced I_{crac}, acidification reduced it. The relation between I_{crac} amplitude and extracellular proton concentration was reversible, and showed a sigmoidal relationship in pH range of 6 to 10 (Fig. 4B). Hill analysis of this relation yielded a pK_a of 7.2 and a Hill coefficient of 1.

Since I_{crac} was nearly abolished at external pH < 6.5, the pH dependence of NPPB inhibition could be investigated with clarity only at alkaline and near neutral pH values. Fig. 5 summarizes the results of inhibition on I_{crac} by NPPB at extracellular pH 7.4 and 8.5. The pH response was first established for each cell, and the fractional I_{crac} block produced by 30 μM NPPB was then measured at each pH and compared. At pH 7.4, NPPB reduced I_{crac} by ~80%; however, when the pH was raised to 8.5, the inhibition was drastically reduced to $< 20\%$. As shown in the same figure, a nearly identical pH-related change in the inhibitory activity of ochratoxin A (100 μM) was demonstrable in a set of separate experiments. In contrast, the quaternary salt econazole methiodide (50 μM; Christian et al., 1996b) showed no statistically significant difference in its inhibitory activity at these two pH values.

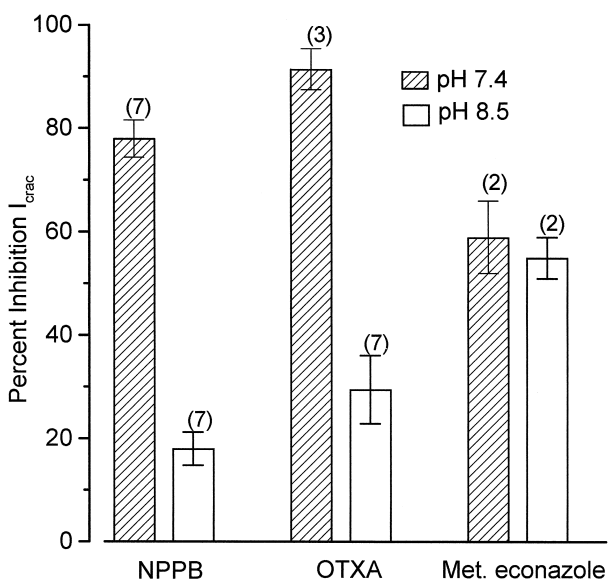

Fig. 5. Effect of external pH on the fractional inhibition of I_{crac} produced by 30 μM NPPB, 100 μM ochratoxin A (OTXA), and 50 μM econazole methiodide (Met. econazole). Each bar represents the mean ± S.E.M. (n in parentheses) percentage inhibition of the Control I_{crac} magnitude at the indicated pH observed in presence of the compound at the same pH. Statistically significant differences were noted only for NPPB and OTXA.

4. Discussion

4.1. Nature of the NPPB interaction with CRAC channels in the Jurkat cell

NPPB, a prototypical Cl^- channel blocker, was first shown to inhibit I_{crac} in human endothelial cells (Gericke et al., 1994) and later in the rat mast cells (Reinsprecht et al., 1995). Available biophysical and pharmacological studies support that I_{crac} in these cell types is virtually indistinguishable from that in the Jurkat cell (for review, see Lewis, 1999), with one exception being that the CRAC channel in the mast cell has been reported to differ somewhat in terms of Ba^{2+} permeability from that in the Jurkat cell (Hoth, 1995). Nonetheless, our results here extend the evidence of a common pharmacological profile of I_{crac} in these different cell types, since NPPB inhibited I_{crac} in the Jurkat cell with a potency analogous to that with which it affects I_{crac} in the other cells.

The rate of I_{crac} block by NPPB was linearly related to concentration (Fig. 2C), as would be predicted for a 1:1 drug to channel interaction. In addition, we showed that I_{crac} amplitude increases to increasing extracellular $[Ca^{2+}]$ in a saturable manner (Fig. 3), confirming prior observations in mast cells (Hoth and Penner, 1993) and Jurkat cells (Premack et al., 1994). Quantitatively, the relation between extracellular $[Ca^{2+}]$ and I_{crac} is well described by a Michaelis–Menten single-site fit, consistent with the idea of a specific Ca^{2+} binding site within the permeation pathway of the CRAC channel. This, taken together with our evidence that increasing extracellular $[Ca^{2+}]$ competitively reduced NPPB-mediated block of I_{crac} (Fig. 3), is consistent with an interesting hypothesis that NPPB blocks the CRAC channel by competing with Ca^{2+} for a specific binding site in the permeation pathway. More conclusive support of this hypothesis would rely on approaches such as molecular structure-function studies based on mutagenesis of targeted residues. Such approaches are obviously inaccessible at present because of a lack of a cloned CRAC channel entity.

4.2. Comparison of NPPB blocking mechanisms of CRAC and $I_{Cl(vol)}$ channels

In view of the above evidence supporting a direct interaction of NPPB in the pore of the CRAC channel, it is worth considering available information about NPPB block of $I_{Cl(vol)}$. Several studies demonstrate that NPPB block of $I_{Cl(vol)}$ in cell types other than Jurkat cells is not voltage-dependent (Schmid et al., 1998; Von Weikersthal et al., 1999). This suggests that NPPB, which is predominantly ionized at physiological pH (Wangemann et al., 1986), is not sensed by the membrane charge field, and thus presumably not exerting block at the pore. Alternatively, the minor uncharged species constitutes the active blocking particle for $I_{Cl(vol)}$, as our data suggest is the case for the CRAC channel (see below). In this regard, technical feasibility problems associated with measurement of small I_{crac} amplitude at depolarized potentials precluded a reasonable experimental evaluation of voltage dependence of I_{crac} block, but if these data had been attainable, they may be predicted to reflect an apparent lack of voltage dependence for I_{crac} due to the uncharged nature of the active blocking particle. In conclusion, even though available reports suggest, based on lack voltage dependency, that NPPB does not block in the permeation pathway of the channel mediating $I_{Cl(vol)}$, additional experiments analogous to those conducted here for the CRAC channel would be beneficial to more definitively compare the NPPB blocking mechanisms of these two channel types.

4.3. Is I_{crac} inhibition by NPPB secondary to Cl^- channel blockade?

Since NPPB as well as several other Cl^- channel blockers also demonstrate inhibitory activity at I_{crac}, the possibility deserves consideration that inhibition of the CRAC channel may be an indirect secondary consequence of Cl^- channel blockade. One piece of evidence arguing against this generalized suggestion is that the Cl^- channel blocker, 4,4′-diisothiocyanatostilbene-2,2-disulphonic acid (DIDS), although ineffective in inhibiting I_{crac}, blocks completely the Cl^- current in rat mast cells (Reinsprecht et al., 1995). However, DIDS may be an exception, since it is structurally quite dissimilar to NPPB, and furthermore, is rather promiscuous with demonstrated inhibitory activity on Na^+ current in guinea pig ventricular myocytes (Liu et al., 1998). On the other hand, ochratoxin A, a closer analog of NPPB, has been reported to be nearly 20 times more potent than NPPB for blocking the plasma membrane anion conductance in Madin–Darby canine kidney epithelial cells in vitro (Gekle et al., 1993). Likewise, we have demonstrated that in Jurkat cells, ochratoxin A is indeed also more potent than NPPB in blocking $I_{Cl(vol)}$ (Li et al., 1997). Thus, if I_{crac} inhibition were simply a secondary consequence of Cl^- channel blockade, a more potent inhibition of I_{crac} by ochratoxin A than by NPPB would be anticipated. On the contrary, ochratoxin A was *less* potent in blocking I_{crac} than NPPB (Fig. 6). This clear separation of rank order potencies of these agents for Cl^- vs. CRAC channel block supports that the inhibition of I_{crac} by NPPB involves a mechanism separable from its Cl^- channel blocking activity. Thus, even in biochemical or pharmacological studies with cells or whole tissues where the cell membrane potential is not clamped, the inhibition of I_{crac} by NPPB is likely attributable to mechanisms aside from, or in addition to, a simple reduction of the driving force on Ca^{2+} as a result of Cl^- channel blockade.

4.4. pH modulation of NPPB blockade

The pH modulation of I_{crac} in Jurkat cells resembles that described for the Ca^{2+} currents activated through depletion of intracellular Ca^{2+} stores in human macrophages (Malayev and Nelson, 1995). The rapid and reversible action of extracellular proton concentration changes on I_{crac} in Jurkat cells would suggest that protons interact at an external site of the CRAC channel. Consistent with this, we have observed that acidifying the intracellular contents to pH 6.5 via the pipette solution does not affect I_{crac} density relative to the normal intracellular pH 7.2 (unpublished data). A similar conclusion of the sites of action of protons on I_{crac} in macrophages was arrived at based upon an observed lack of effect of intracellular pH

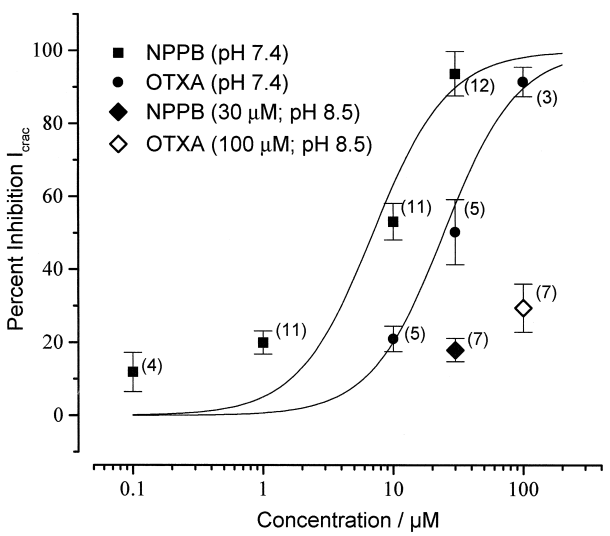

Fig. 6. Concentration–response relationships for I_{crac} inhibition by NPPB and OTXA at external pH 7.4, and the percentage inhibition of I_{crac} measured to the indicated single concentrations of NPPB and OTXA at pH 8.5 (diamonds). Note that based on the pK_a values of 4.5 for NPPB and 7.04 for OXTA, the concentrations of the neutral form of these at the pH 8.5 test point would be equivalent to the concentration of neutral species present at pH 7.4 in 2.5 μM NPPB and 10 μM OTXA, respectively. These predicted concentrations of the uncharged species at pH 8.5 would yield a percentage inhibition (based on the full concentration–response curves at pH 7.4) that is commensurate with the observed inhibition for 30 μM NPPB and 100 μM OTXA at this higher pH (see text).

buffering capacity on the extracellular proton-induced blockade of the current (Malayev and Nelson, 1995). Nonetheless, a recent report indicates that intracellular acidification can influence the kinetics of CRAC channels as well as block the Ca^{2+} current through these channels (Kerschbaum and Cahalan, 1998).

As demonstrated recently, under conditions where extracellular Ca^{2+} and Mg^{2+} are reduced to micromolar levels, the previously highly Ca^{2+} selective CRAC channel becomes permeable to monovalent Na^{+} (Lepple-Wienhues and Cahalan, 1996). We have noted that under conditions which promote Na^{+} permeation through I_{crac}, a pH modulation of current analogous to that observed with Ca^{2+} as the charge carrier occurs (Li et al., 1998). This further supports the idea that the CRAC channel, like many other ion channel types, is subject to modulation by protons.

The pH dependence of NPPB or ochratoxin A mediated I_{crac} inhibition appeared similar. Since alkalinization of extracellular media increased I_{crac}, this increased signal-to-noise discrimination would, in principle, facilitate the measurement of the inhibitory activity of blockers. Nonetheless, we found that the inhibition of I_{crac} by a near-maximal concentration of either NPPB and ochratoxin A was decreased substantially when the extracellular pH increased from 7.4 to 8.5. A possible explanation for this reduction of inhibitory activity of ochratoxin A and NPPB is that the neutral form of these molecules represents the active species for blocking the channel. Both NPPB and ochratoxin A bear a carboxylic group and have pK_a values of 4.5 (Wangemann et al., 1986; Walsh and Wang, 1998) and ~ 7 (Chu, 1971), respectively. Therefore, even though NPPB is a stronger acid as compared to ochratoxin A, the ionized form of either of these would predominate at pH 7.4. As the external medium pH increases from 7.4 to 8.5, the fraction of the ionized form of either compound would increase further, and the neutral form would decrease accordingly. Hypothetically, the reduction of I_{crac} inhibition by either ochratoxin A or NPPB at a more alkaline pH thus may be directly attributable to the decrease of the neutral form of the blocker in the medium. More specifically, the concentration of the neutral form of 100 μM ochractoxin A at pH 8.5 is about the same as the concentration that would be present in a 10-μM ochratoxin A solution at pH 7.4. Likewise, 30 μM NPPB at pH 8.5 would yield a concentration of neutral species similar to that of 2.5 μM NPPB at pH 7.4. Indeed, as shown in Fig. 6, the magnitudes of the inhibition of I_{crac} produced at pH 8.5 by 100 μM ochratoxin and 30 μM NPPB were comparable to the levels of inhibition measured at pH 7.4 with 10 μM ochratoxin and 3 μM NPPB, in accordance with the predicted equivalent concentrations of neutral species under the two pH conditions.

To test further the hypothesis that the neutral species of these acidic blockers represent the active forms responsible for inhibiting I_{crac}, it would have been desirable to determine whether increased inhibition could be recorded at acidic pH. This was technically not feasible, since acidification itself nearly eliminated I_{crac}. We therefore chose instead to compare the effect of alkaline pH on the inhibitory activity of a basic I_{crac} blocker, econazole methiodide, for which the neutral form of the molecule would predominate at the two pH values tested. Previously, this quaternary salt of econazole at 30 μM and pH 7.4 was shown to block I_{crac} $\sim$40% (Christian et al., 1996b). In the present study, 50 μM econazole methiodide blocked I_{crac} by $\sim$60% at extracellular pH 7.4 as well as 8.5. The lack of significant pH dependence of this inhibition by the basic econazole methiodide is consistent with the idea that the neutral form of this molecule, as with NPPB, also is likely the active species.

In conclusion, we have provided a variety of convergent experimental evidence supporting a hypothesis that the potent chloride channel blocker, NPPB, interacts directly to inhibit calcium flux through the CRAC channel with potency comparable to that producing chloride channel blockade. This information may thus provide an impetus to use NPPB as a chemical starting point to design more selective CRAC vs. chloride channel antagonists. Importantly, however, our findings also highlight that caution must be applied in associating cellular and physiological effects with chloride channel blockade as a result of pharmacological manipulations with NPPB and structurally analogous compounds.

References

Barry, P.H., Lynch, J.W., 1991. Liquid junction potentials and small cell effects in patch clamp analysis. J. Membr. Biol. 121, 101–117.

Christian, E.P., Spence, K.T., Togo, J.A., Dargis, P.G., Patel, J., 1996a. Calcium-dependent enhancement of depletion-activated calcium current in Jurkat T lymphocytes. J. Membr. Biol. 150, 63–71.

Christian, E.P., Spence, K.T., Togo, J.A., Dargis, P.G., Warawa, E., 1996b. Extracellular site for econazole-mediated block of Ca^{2+} release-activated Ca^{2+} current (I_{crac}) in T lymphocytes. Br. J. Pharmacol. 119, 647–654.

Chu, F.S., 1971. Interaction of ochratoxin A with bovine serum albumin. Arch. Biochem. Biophys. 147, 359–366.

Chung, S.C., McDonald, T.V., Gardner, P., 1994. Inhibition by SK&F 96365 of Ca^{2+} current, IL-2 production and activation in T lymphocytes. Br. J. Pharmacol. 113, 861–868.

Gekle, M., Oberleithner, H., Silbernagl, S., 1993. Ochratoxin A impairs ''postproximal'' nephron function in vivo and blocks plasma membrane anion conductance in Madin–Darby canine kidney cells in vitro. Pflügers Arch. 425, 401–408.

Gericke, M., Oike, M., Droogmans, G., Nilius, B., 1994. Inhibition of capacitative Ca^{2+} entry by a Cl^{-} channel blocker in human endothelial cells. Eur. J. Pharmacol. 269, 381–384.

Greger, R., Nitschke, R.B., Lohrmann, E., Burhoff, I., Hropot, M., Englert, H.C., Lang, H.J., 1991. Effects of arylaminobenzoate-type chloride channel blockers on equivalent short-circuit current in rabbit colon. Pflügers Arch. 419, 190–196.

Greger, R., Schlatter, E., Gögelein, H., 1987. Chloride channels in the luminal membrane of the rectal gland of the dogfish (*Squalus acanthias*). Properties of the ''larger'' conductance channel. Pflügers Arch. 409, 114–121.

Gschwentner, M., Jungwirth, A., Hofer, S., Wöll, E., Ritter, M., Susanna, A., Schmarda, A., Reibnegger, G., Pinggera, G.M., Leitinger, M., Frick, J., Deetjen, P., Paulmichl, M., 1996. Blockade of swelling-induced chloride channels by phenol derivatives. Br. J. Pharmacol. 118, 41–48.

Hamill, O.P., Marty, A., Neher, E., Sakmann, B., Sigworth, F.J., 1981. Improved patch-clamp techniques for high-resolution recording from cells and cell-free membrane patches. Pflügers Arch. 391, 85–100.

Heinke, S., Szücs, G., Norris, A., Droogmans, G., Nilius, B., 1995. Inhibition of volume-activated chloride currents in endothelial cells by chromones. Br. J. Pharmacol. 115, 1393–1398.

Hoth, M., 1995. Calcium and barium permeation through calcium release-activated calcium (CRAC) channels. Pflügers Arch. 430, 315–322.

Hoth, M., Penner, R., 1993. Calcium release-activated calcium current in rat mast cells. J. Physiol. 465, 359–386.

Kerschbaum, H.H., Cahalan, M.D., 1998. Monovalent permeability, rectification, and ionic block of store-operated calcium channels in Jurkat T lymphocytes. J. Gen. Physiol. 111, 521–537.

Kerschbaum, H.H., Cahalan, M.D., 1999. Single-channel recording of a store-operated Ca^{2+} channel in Jurkat T lymphocytes. Science 283, 836–839.

Lepple-Wienhues, A., Cahalan, M.D., 1996. Conductance and permeation of monovalent cations through depletion-activated Ca^{2+} channels (I_{crac}) in Jurkat T cells. Biophys. J. 71, 787–794.

Lewis, R.S., 1999. Store-operated calcium channels. Adv. Second Messenger Phosphoprotein Res. 33, 279–307.

Lewis, R.S., Ross, P.E., Cahalan, M.E., 1993. Chloride channels activated by osmotic stress in T lymphocytes. J. Gen. Physiol. 101, 801–826.

Li, J.H., Dargis, P.G., Togo, J.A., Spence, K.T., Christian, E.P., 1997. Inhibition of Ca^{2+} release-activated Ca^{2+} current (Icrac) in Jurkat cells by ochratoxin. The Pharmacologist 39, 59.

Li, J.H., Dargis, P.G., Togo, J.A., Spence, K.T., Christian, E.P., 1998. pH dependence of Ca^{2+} release-activated Ca^{2+} current (I_{crac}) and its blockade in Jurkat cells. FASEB J. 12, A440.

Li, J.H., Kau, S.T., 1987. Amphibian cornea as a model for studying intrinsic activities of loop diuretics. J. Pharmacol. Methods 18, 283–294.

Liu, J., Lai, Z.F., Wang, X.D., Tokutomi, N., Nishi, K., 1998. Inhibition of sodium current by chloride channel blocker 4,4′-diisothiocyanatostibene-2,2′-disulfonic acid (DIDS) in guinea pig cardiac ventricular cells. J. Cardiovasc. Pharmacol. 31, 558–567.

Malayev, A., Nelson, D.J., 1995. Extracellular pH modulates the Ca^{2+} current activated by depletion of intracellular Ca^{2+} stores in human macrophages. J. Membr. Biol. 146, 101–111.

McCann, J.D., Li, M., Welsh, M.J., 1989. Identification and regulation of whole-cell chloride currents in airway epithelium. J. Gen. Physiol. 94, 1015–1036.

McDonald, T.V., Premack, B.A., Gardner, P., 1993. Flash photolysis of a caged inositol 1,4,5-trisphosphate activates plasma membrane calcium current in human T cells. J. Biol. Chem. 268, 3889–3896.

Nilius, B., Sehrer, J., Viana, F., De Greef, C., Raeymaekers, L., Eggermont, J., Droogmans, G., 1994. Volume-activated Cl^- currents in different mammalian non-excitable cell types. Pflügers Arch. 428, 364–371.

Premack, B.A., McDonald, T.V., Gardner, P., 1994. Activation of Ca^{2+} current in Jurkat T cells following the depletion of Ca^{2+} stores by microsomal Ca^{2+}-ATPase inhibitors. J. Immunol. 152, 5226–5240.

Reinsprecht, M., Rohn, M.H., Spadinger, R.J., Pecht, I., Schindler, H., Romanin, C., 1995. Blockade of capacitive Ca^{2+} influx by Cl^- channel blockers inhibits secretion from rat mucosal-type mast cells. Mol. Pharmacol. 47, 1014–1020.

Schmid, A., Blum, R., Krause, E., 1998. Characterization of cell volume-sensitive chloride currents in freshly prepared and cultured pancreatic acinar cells from early postnatal rats. J. Physiol. 513, 453–465.

Schumacher, P.A., Sakellaropoulos, G., Phipps, D.J., Schlichter, L.C., 1995. Small-conductance chloride channels in human peripheral T lymphocytes. J. Membr. Biol. 145, 217–232.

Spence, K.T., Dargis, P.G., Christian, E.P., 1996. NPPB blocks volume-regulated chloride current and capacitive calcium current in Jurkat cells. Biophys. J. 70, A324.

Von Weikersthal, S.F., Barrand, M.A., Hladky, S.B., 1999. Functional and molecular characterization of a volume-sensitive chloride current in rat brain endothelial cells. J. Physiol. 516, 75–84.

Walsh, K.B., Wang, C., 1998. Arylaminobenzoate block of the cardiac cyclic AMP-dependent chloride current. Mol. Pharmacol. 53, 539–546.

Wangemann, P., Wittner, M., Di Stefano, A., Englert, H.C., Lang, H.J., Schlatter, E., Greger, R., 1986. Cl^- channel blockers in the thick ascending limb of the loop of Henle. Structure activity relationship. Pflügers Arch. 407, S128–S141.

Zweifach, A., Lewis, R.S., 1993. Mitogen-regulated Ca^{2+} current of T lymphocytes is activated by depletion of intracellular Ca^{2+} stores. PNAS 90, 6295–6299.